Three species multiplexing of fluorescent dyes and gold nanoclusters recovered with fluorescence lifetime correlation spectroscopy

Malavika Kayyil Veedu, Agata Hajda, Joanna Olesiak-Bańska, Jérôme Wenger

BBA - General Subjects 1868 (2024) 130611

Contents lists available at ScienceDirect

BBA - General Subjects

journal homepage: www.elsevier.com/locate/bbagen

Three species multiplexing of fluorescent dyes and gold nanoclusters recovered with fluorescence lifetime correlation spectroscopy

Malavika Kayyil Veedu [a], Agata Hajda [b], Joanna Olesiak-Bańska [b], Jérôme Wenger [a,*]

[a] Aix Marseille Univ, CNRS, Centrale Med, Institut Fresnel, AMUTech, 13013 Marseille, France
[b] Institute of Advanced Materials, Wroclaw University of Science and Technology, Wrocław, Poland

ARTICLE INFO

Keywords:
Fluorescence lifetime correlation spectroscopy
FLCS
Gold nanoclusters
Fluorescence multiplexing
Fluorescence sensing

ABSTRACT

Biosensor applications often require the simultaneous detection of multiple analytes, with a clear need to go beyond the traditional multiplexing relying on distinct fluorescent dyes across the visible spectrum. Fluorescence lifetime correlation spectroscopy (FLCS) is a powerful approach taking advantage of the fluorescence lifetime information to separate the contributions of different fluorescent species with overlapping emission spectra. However, so far FLCS detection has been demonstrated only on binary mixtures of two fluorescent dyes, limiting its multiplexing capabilities. Here, we report the first quantitative FLCS measurements within a ternary mixture composed of three different fluorescent emitters with near-identical emission spectra. Two organic fluorescent dyes, Alexa Fluor 647 and CF640R, are combined with water-soluble $Au_{18}(SG)_{14}$ gold nanoclusters. Our experimental data establish that FLCS allows to accurately determine individual concentrations within intricate ternary mixtures. Another major aspect of interest concerns the assessment of the suitability of gold nanoclusters for FLCS multiplexing applications. With their microsecond lifetime and stable emission characteristics, gold nanoclusters add a valuable new aspect to the array of FLCS probes. Extending FLCS multiplexing beyond binary mixtures paves the way for further progress in the simultaneous highly parallel biosensing of multiple species.

1. Introduction

Single molecule sensors and related techniques have garnered increasing attention in the biological study of nucleic acids and proteins [1,2]. Among the different fluorescence-based single molecule techniques, fluorescence correlation spectroscopy (FCS) stands out as a well-established and versatile tool, allowing for the precise measurement of local concentrations, diffusion coefficients, and biochemical reaction rates [3–5]. For biosensors, the simultaneous detection and analysis of multiple analytes in parallel is a highly coveted capability [6], as it allows to gain in specificity, selectivity, read-out time and overall accuracy. The majority of multiplexing applications in fluorescence sensing have traditionally relied on distinct organic fluorescent dyes spanning the blue, green, orange, and red regions of the electromagnetic spectrum [7,8]. In the context of FCS, the use of spectrally different fluorescent dyes has given rise to fluorescence cross-correlation spectroscopy (FCCS) [9,10] enabling the simultaneous monitoring of up to four distinct species and colors [11]. However, for advanced applications it is often necessary to go beyond the typical 4 colors combination [12,13]. For instance, 22 different aminoacids need to be distinguished in protein sequencing, requiring multiple optical readouts that transcend the standard fluorescence spectrum [14,15].

The introduction of the fluorescence lifetime is a major supplementary parameter to distinguish between different fluorophores based on their emission dynamics in the time domain rather than in the spectral domain [16–19]. Within the realm of FCS, the use of the supplementary lifetime information has paved the way for the development of fluorescence lifetime correlation spectroscopy (FLCS) [20–23]. In FLCS, the fluorescence lifetime information serve to filter the raw detected fluorescence intensity time trace and compute lifetime-specific correlation functions. FLCS is an extension and a generalization of time-gated FCS [24], and has proven particularly invaluable in distinguishing two species within a mixture [20,21,25,26], correcting for a non-correlating background [21,27] or removing afterpulsing artefacts in the correlation data [28]. However, while the ability of FLCS to distinguish two species has been well characterized [20,21,25,26], the extension of FLCS for multiplexing involving three species or more has not been documented yet.

Achieving multiplexing in FLCS necessitates the use of fluorescent labels with substantial differences in their emission lifetimes. With their

* Corresponding author.
E-mail address: jerome.wenger@fresnel.fr (J. Wenger).

https://doi.org/10.1016/j.bbagen.2024.130611
Received 18 December 2023; Accepted 26 March 2024
Available online 28 March 2024

photoluminescence lifetimes in the tens of nanosecond range, quantum dots might initially seem like a natural choice, yet their complex blinking dynamics [29,30] and their multi-exponential lifetime decays [31–33] may complicate the FLCS analysis. As an alternative to colloidal semiconductor quantum dots, gold nanoclusters are gaining attention, despite the limited knowledge available regarding their application in FCS [27,34]. Gold nanoclusters (AuNCs) are metal nanoparticles composed of metal core with surface stabilized with ligands, usually thiols. Atomically precise AuNCs are characterized by a exact number of gold atoms and ligand molecules and a diameter below 2 nm [35–38]. They constitute a bridge between plasmonic metal nanoparticles and simple molecules, which results in discrete electronic structures and distinctive optical properties, notably size and structure-dependent visible to near-infrared photoluminescence and long photoluminescence lifetimes in the microsecond range [39–41]. While AuNCs have found utility in a range of applications spanning catalysis [42,43], optical devices [44–46], biosensing [47], and bioimaging [48–50], their application in the domain of FLCS multiplexing remains an uncharted territory.

Here, we report the first quantitative FLCS measurements within a ternary mixture composed of three different fluorescent emitters with near-identical emission spectra. Specifically, we combine two organic fluorescent dyes, Alexa Fluor 647 and CF640R, with water-soluble $Au_{18}(SG)_{14}$ nanoclusters (where SG denotes L-glutathione) in varying proportions. Our experimental findings unequivocally demonstrate that FLCS filtering enables the precise determination of individual concentrations and diffusion times for each of the three constituent species. This demonstration not only marks a pivotal advancement toward future developments in FLCS multiplexing for biosensing applications, but also serves as a critical assessment of the utility and applicability of AuNCs in FLCS investigations. In stark contrast to spectral multiplexing employed in FCCS, which necessitates the use of complex instrumentation featuring various laser lines and detection channels [10,11], our 3-species lifetime multiplexing relies solely on a single laser line and a single pinhole detection. This results in a significant simplification of the microscope setup, underscoring the practical advantages of FLCS multiplexing.

2. Materials and methods

2.1. Sample preparation

Alexa Fluor 647 and CF640R dyes are purchased from Thermofisher and Sigma-Aldrich respectively and used as received. Gold nanoclusters are synthesized using the protocol detailed in Ref. [51]. 100 mg of L-glutathione (GSH), 0.4 mL of methanol and 0.4 mL of water are mixed in 25 mL round flask. $HAuCl_4{*}3H_2O$ is added (200 μL, 0.6362 M) after a few minutes and mixed for 10 min. The solution is then diluted with methanol to 10 mL and a slow reduction is performed using methanolic solution of $NaBH_3CN$ (1.5 mL, 220 mM) for 1 h. The reaction mixture was centrifuged (10 min/12000 rpm). Supernate is collected and precipitated by MeOH through centrifugal precipitation (10 min/12000 rpm). The collected sediment is dissolved in water and washed three times with methanol/ethanol, each time centrifuged (10 min/12000 rpm) to remove the remaining reaction precursors. All used reagents for synthesis for AuNC were purchased from Sigma-Aldrich. All the dilutions for the FLCS experiments are done in D_2O, purchased from Sigma-Aldrich.

2.2. FLCS setup

The sample solution is excited at 557 nm by a pulsed laser (iChrome-TVIS laser, Toptica GmbH, pulse duration ~3 ps) with a repetition rate of 40 MHz and a power of 20 μW. A multiband dichroic mirror (ZT 405/488/561/640rpc, Chroma) and a Zeiss C-Apochromat 63×, 1.2 NA water immersion objective lens are used to reflect laser toward the microscope and focus the excitation light respectively. The emission is collected by the same objective lens in the epifluorescence configuration. An emission filter (ZET405/488/565/640mv2, Chroma) is used to block the laser back reflection. The fluorescence signal is focused onto an 80 μm pinhole. The emitted photons in the 650–750 nm spectral range are recorded by two avalanche photodiodes APDs (Perkin Elmer SPCM-AQR-13) separated by a 50/50 beam-splitter in a Hanbury-Brown-Twiss configuration. A time-correlated single photon counting (TCSPC) module (HydraHarp 400, Picoquant) records the arrival time of each fluorescence photon in a time-tagged time-resolved (TTTR) mode. The integration time for each FLCS experiment is 20 min.

2.3. FLCS analysis

The FLCS analysis is implemented using the software Symphotime64 (Picoquant). For a 3-component mixture, the fluorescence lifetime decay curve of the mixture, $D(i)$ can be expressed as a linear combination as given by Eq. (1)

$$D(i) = \omega_A\, d_A(i) + \omega_B d_B(i) + \omega_C\, d_C(i) \tag{1}$$

where ω is the photon count amplitude (in number of photons) and d is the normalized TCSPC decay pattern of each species [20,21]. Here the index i is the channel number for the photons detected within the TCSPC channel. Then a statistical filter function, $f(i)$ is introduced that can satisfy the following requirements

$$\sum f(i) \times D(i) = \omega \tag{2}$$

$$f^A + f^B + f^C = 1 \tag{3}$$

Based on the TCSPC histogram, these filter functions can be calculated numerically. The filter functions corresponding to the different species are obtained experimentally by fitting the TCSPC pattern of the mixture (Fig. 2a,b), taking into account the instrument response function (IRF) computed by the Symphotime64 software from the rise time on the TCSPC histogram. For the TCSPC fitting, we set the fluorescence lifetime to 1.3 and 4.2 ns, which correspond to the lifetimes recorded for pure Alexa647 and CF640R solutions (Fig. 1d). The contribution for the AuNCs is retrieved from the flat contribution (so-called "background" in the software, which also includes the scattering peak) as the fluorescence lifetime of gold nanoclusters is on the order of a microsecond [34]. Examples of filter functions are shown on Fig. 2b with their corresponding TCSPC histogram in Fig. 2a.

The correlation functions are then obtained using [20,21].

$$G(\tau) = \frac{\langle \sum_i f_i I_i(t) \times \sum_i f_i I_i(t+\tau) \rangle}{\langle \sum_i f_i I_i(t) \rangle^2} \tag{4}$$

This correlation is fitted using the dark state blinking model [3] given by

$$G(\tau) = \frac{1}{N}\left(1 + \frac{\tau}{\tau_D}\right)^{-1} \times \left(1 + \frac{\tau}{\tau_D \kappa^2}\right)^{-1/2} \times \left(1 + \frac{T}{1-T} exp\left(\frac{-\tau}{\tau_{DS}}\right)\right) \tag{5}$$

where $G(\tau)$ is the cross-correlation function at time τ, N is the total number of molecules in the observation volume, τ_D is the mean diffusion time, T is the fraction of molecules in the dark state, τ_{DS} is the dark state blinking time and κ denotes the aspect ratio of the axial to the transversal dimension of the detection volume. Here κ is taken as 5 based on our past confocal results and fits well with our experimental correlation data.

The lifetimes for the Alexa647 and CF640R dyes differ significantly from the background, and as a result of the FLCS treatment, the scattering background does not influence the FLCS data for these dyes. However, the long photoluminescence lifetime of the AuNC cannot be distinguished from the flat background contribution in the TCSPC histogram. To estimate the number of molecules for the AuNC, we correct

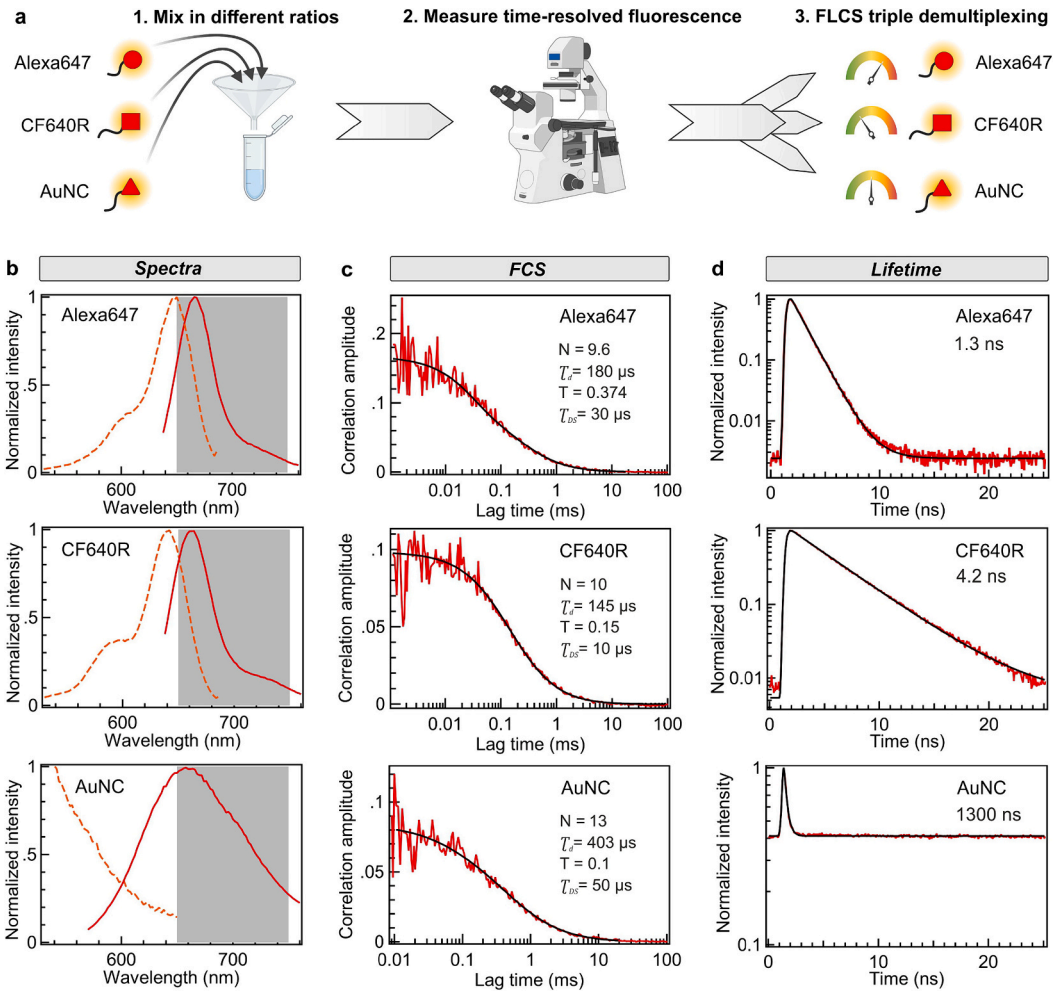

Fig. 1. (a) Concept of the experiment: three different fluorescent dyes of similar spectra but different lifetimes are mixed with varying ratios. Time-resolved confocal measurements followed by FLCS data analysis allow to recover the concentration and diffusion time of each individual species. (b) Fluorescence excitation (dashed line) and emission (solid line) spectra for the three different dyes. The shadow area indicates the 650–750 nm spectral range used for detection. (c) FCS correlation data and fit results for the pure species taken individually in a 10 nM solution. (d) Fluorescence decay traces and single exponential fit result taking into account the convolution with the instrument response function (IRF). The peak seen at 1 ns on the AuNC data corresponds to the background contribution of laser backscattering and Raman scattering.

for the background by adding an extra correction term $\left(1-\frac{B}{I_{NC}}\right)^2$ to Eq. (5) as commonly done in regular FCS [3,26]. B is the background intensity level measured to be 515 counts/s for pure D_2O (corresponding essentially to the sum of the dark counts of the two avalanche photodiodes). I_{NC} is the total fluorescence intensity attributed to the AuNC and background component, calculated as $I_{NC}=\frac{C\times n}{T_{int}}$ where C is the baseline counts per TCSPC channel recorded for each mixture, $n=395$ is the number of TCSPC channels in our experiments and T_{int} is the total integration time for each experiment.

3. Results

We start by characterizing each species individually. All our experiments are performed in deuterated water D_2O to maximize the fluorescence brightness and avoid fluorescence quenching by the residual absorption of water molecules, as demonstrated in Ref. [52,53]. Alexa647, CF640R and AuNC have nearly overlapping fluorescence emission spectra (Fig. 1b), making these emitters spectrally quasi-undistinguishable. Standard FCS struggles to distinguish these emitters (Fig. 1c), as their respective diffusion times are close to each other. On the contrary, the TCSPC histograms show a remarkable difference between the species (Fig. 1d): Alexa647 has a 1.3 ns lifetime while CF640R lifetime is 4.2 ns and the AuNCs have a long photoluminescence lifetime of 1.3 μs, appearing nearly as a flat line within the 25 ns (=1/40 MHz, inverse of the laser repetition rate) window of our TCSPC instrument. We have recently published a study investigating the emission photophysics of AuNCs probed by FCS [34]. It was found that the gold nanoclusters exhibited minimal blinking, with blinking amplitudes T well below 0.2, in stark contrast to DNA-encapsulated silver nanoclusters. The observation of photon antibunching in the FCS correlation at lag times below 1 μs showcased the quantum nature of the emission process [34], establishing each AuNC as an individual quantum source. Altogether, these preliminary FCS investigations of AuNCs indicate a good potential of AuNCs for new fluorescence probes in FCS applications.

In the following, we focus on FLCS demultiplexing within ternary mixtures composed of Alexa647, CF640R and AuNCs in different proportions. The mixtures are characterized by a set of three numbers A:B:C where the first number A denotes the relative fraction of Alexa647, the second number B indicates the fraction of CF640R and the last number C is for the gold nanoclusters AuNC. Each initial solution of the pure compound has a concentration of 10 nM, as characterized by standard FCS in Fig. 1c.

Fig. 2 shows typical experimental results for a 4:3:3 mixture composed of 40% Alexa647, 30% CF640R and 30% AuNCs. The TCSPC

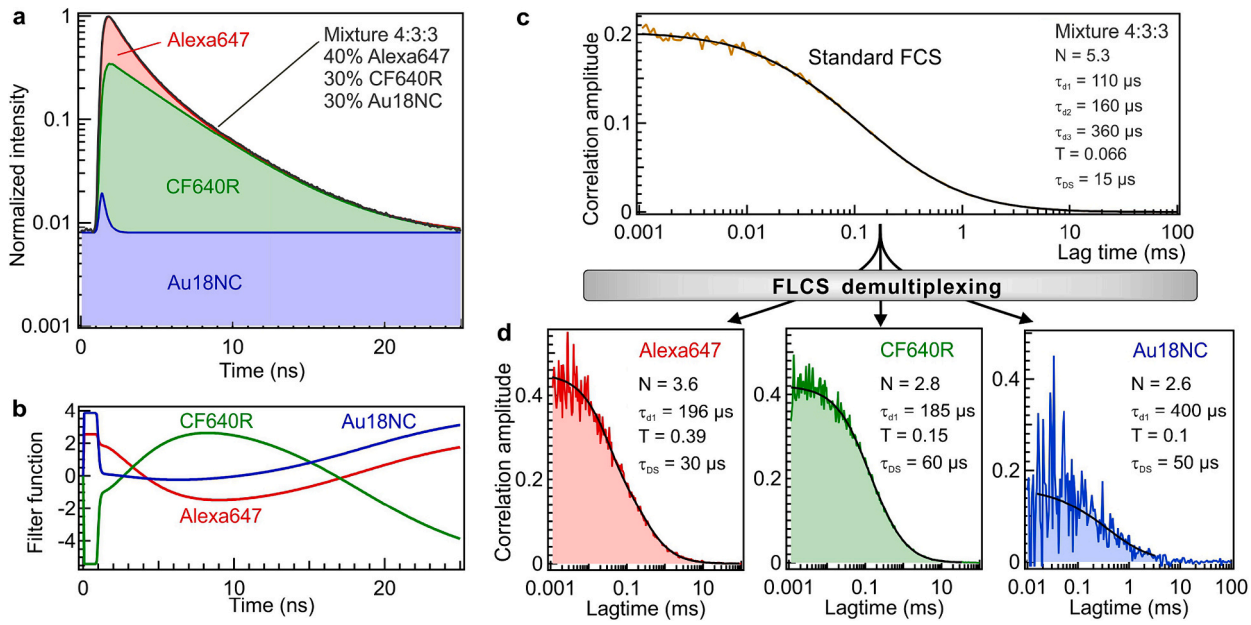

Fig. 2. Example of FLCS demultiplexing for a mixture consisting of 40% Alexa647, 30% CF640R and 30% Au18NC solutions, each species being diluted at a 10 nM concentration. (a) Fluorescence lifetime decay of the mixture, which the contribution of each species being highlighted in a different color. (b) FLCS filter functions calculated from the TCSPC histogram in (a) for each species. (c) Standard FCS correlation of the mixture. (d) FLCS filtered correlations of the same data as in (c) allowing to recover the contributions of each species.

histogram recorded with the mixture (Fig. 2a) can be decomposed as a sum of the contributions of each species, as highlighted by the colored regions. Fitting this TCPSC histogram with the known lifetimes of Alexa647 and CF640R (from Fig. 1d) and a flat baseline (for the AuNC contribution) provides the FLCS filter functions displayed in Fig. 2b. Fig. 2c shows the correlation data obtained using standard FCS on this 4:3:3 mixture, together with a numerical fit considering three distinct species. For standard FCS performed on a mixture, the correlation contribution of each species is weighted by the square of its respective fluorescence brightness [3]. Here our emitters have significantly different brightness: a single Alexa647 molecule emits 2 kcounts/s, CF640R 3.6 kcounts/s and AuNCs 0.3 kcounts/s. Therefore, retrieving the different contributions is very challenging for standard FCS. Here a total number of 5.3 molecules is determined from standard FCS, yet this number is quite unrelated to the real number of molecules for each individual species. FLCS filtering is a better approach to recover the respective contributions for each species (Fig. 2d) and assess quantitatively their respective numbers of molecules and diffusion times.

While FLCS has been already reported to distinguish two species of overlapping spectra [20,21,25,26] or one species from the background [21,27], here it is the first time that FLCS is employed for demultiplexing the data in a 3-species mixture and with AuNCs. To assess the performance of the technique and the relevance of AuNCs in this context, we have prepared a series of mixtures with different relative fractions of Alexa647, CF640R and AuNCs (Fig. 3a,b). The respective proportions of each species is varied by up to 6 times between different mixtures to explore a broad range of conditions. As each species has been calibrated separately (Fig. 1c) and as we know the respective dilutions to form the ternary mixtures, we can predict for each case the expected numbers of molecules seen by FLCS for each species and each complex mixture (empty markers in Fig. 3a). This number is then compared to the experimental numbers of molecules measured for each species after FLCS demultiplexing (solid markers in Fig. 3a).

For all the different mixtures and different range of concentrations, we find a good agreement with the measured and expected values for the numbers of molecules of each species (Fig. 3a). The comparison can also be expressed as a function of the respective molecular fraction of each species (Fig. 3b). For a given ternary mixture, the molecular fraction is defined as the number of molecules seen for one species divided by the sum of the numbers of molecules seen for all species:

$$\rho_j = \frac{N_j}{\sum_{k=A,B,C} N_k} \tag{6}$$

Fig. 3b compares the molecular fractions measured by FLCS with the expected values from the dilutions. Again, we find a good agreement for all the different mixtures and species, validating the FLCS approach to recover the respective concentration of each species.

For each measurement of the number of molecules or molecular fraction, the relative error is defined as the difference between the measured value M and the expected value E, divided by the expected value:

$$Relative\ Error = \frac{M - E}{E} \tag{7}$$

The relative errors for the FLCS measurements of the numbers of molecules N and the molecular fractions ρ are represented in Fig. 3c, d respectively. For Alexa647 and CF640R, the average relative errors are $\pm$7% for measurements of the numbers of molecules, and $\pm$ 5% for the molecular fractions. For the gold nanoclusters AuNCs, the relative errors are slightly bigger because of the lower fluorescence brightness and longer lifetime. We find an average relative error of $\pm$22% for the numbers of molecules, and $\pm$ 13% for the molecular fractions in the case of AuNCs. Improving the AuNC luminescence brightness by ligand exchange [34,54], reducing the background intensity and/or increasing the total integration time will further promote the accuracies as in regular FCS.

Lastly, the FLCS filters allow us to investigate the cross-talk between different channels and species. In Fig. 3e, we again consider the 4:3:3 mixture analyzed in Fig. 2, and we represent the cross-correlation amplitudes obtained while computing FLCS correlations with different filters. The diagonal terms in Fig. 3e represent the FLCS correlation amplitude while correlating the FLCS filter of the same species (as used in Fig. 2d). The off-diagonal terms in Fig. 3e are the FLCS correlation amplitudes obtained while correlating the filter for one species with the filter of another species (*e.g.* correlating Alexa647 filtered intensity with

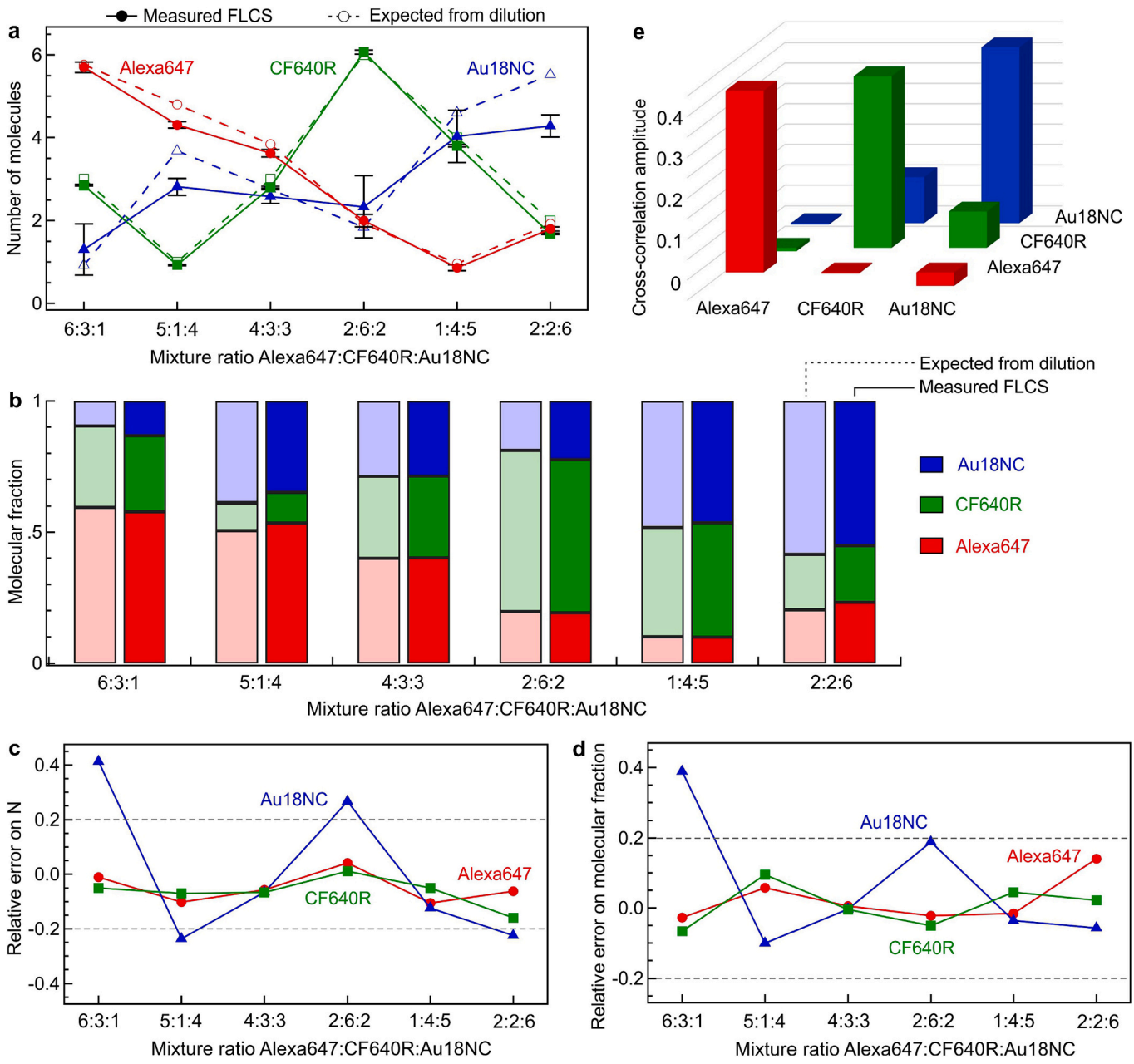

Fig. 3. FLCS demultiplexing of the mixtures allows to quantitatively assess the numbers of molecules of each species. (a) Numbers of molecules measured by FLCS for each species (solid markers). The empty markers indicate the expected result knowing the respective concentrations and mixture ratios. (b) Comparison of the respective fractions for each species measured by FLCS (bright colorbars) and expected from the dilutions (dull pastel colorbars) for the different mixture ratios. (c) Relative error on the measured numbers of molecules in (a) as compared to the expected values. (d) same as (c) for the molecular fractions displayed in (b). (e) Cross-correlation amplitude of the FLCS data for the different filters showing good specificity for the diagonal terms and minimum crosstalk between different components. For this data, we have again considered the 4:3:3 mixture as used in Fig. 2.

AuNC filter intensity). These terms represent the crosstalk between the detection channels. For Alexa647 and CF640R, and for Alexa647 and AuNC, we find negative correlation amplitudes between −0.003 and −0.03, which are dominated by noise and have no physical meaning. These results indicate that the short lifetime of Alexa 647 in the nanosecond range allows for an efficient discrimination of this species with the two others. For CF640R and AuNC, there is a higher cross-correlation amplitude between the species, about 25% of the correlation amplitude found for each species individually. This stems from the longer lifetimes of CF640R and AuNC and the partial overlap of their respective FLCS filters. Despite this partial overlap, the significantly 4× higher correlation amplitude for the diagonal terms in Fig. 3e illustrate the discrimination performance of FLCS in distinguishing different fluorescent species.

4. Discussion

We have detailed the first quantitative FLCS measurements within a ternary mixture composed of three different fluorescent emitters with near-identical emission spectra. Using the lifetime information to filter the fluorescence intensity is a robust and simple approach to parallel detection of multiple species and a significant step forward as compared to conventional FCS or FCCS. Our experimental data clearly establish that FLCS filtering enables the precise determination of individual concentrations within complex ternary mixtures. This demonstration advances FLCS multiplexing for biosensing applications, going well

beyond the usual binary mixtures [20,21,25,26]. The application described here is not restricted to gold nanoclusters, any emitter with significantly long lifetime could be used as well. This includes quantum dots with lifetimes in the tens of nanosecond range [29,31] or nanoparticles doped with lanthanides [55–57].

Furthermore, this study critically assesses the utility and applicability of AuNCs in FLCS investigations. With their long luminescence lifetime in the microsecond range and stable emission properties, gold nanoclusters introduce a valuable dimension to the repertoire of FCS probes. A precise knowledge of their microsecond photoluminescence lifetime is not necessary, as their TCSPC contribution can be reasonably approximated by a flat baseline. While employing AuNCs in FLCS, it becomes necessary to correct for the background contribution, which is not automatically addressed, as is the case with FLCS involving organic dyes with nanosecond lifetimes. The method outlined here, based on the conventional approach to background correction in standard FCS, demonstrates the continued feasibility of accurate concentration measurements using AuNCs, even in complex ternary mixtures with organic fluorescent dyes of overlapping spectra.

From an instrumentation point of view, only a single laser line and a single channel detection are needed. While it should be reminded that FLCS puts more demand on the FLCS electronics, this remains well within reach of modern current electronics. Avoiding the need to overlap different detection volumes as in dual-color FCCS or circumventing the need for two-photon excitation using ultrashort laser pulses are additional advantages of the FLCS multiplexing approach.

In summary, our study represents a significant advancement in the field of FLCS multiplexing for biosensing applications, extending the method beyond binary mixtures. The utility of AuNCs has been critically assessed, and the simplicity of our approach in terms of instrumentation is a noteworthy advantage. As such, this research lays the foundation for further progress in the simultaneous parallel FLCS detection of multiple species.

CRediT authorship contribution statement

Malavika Kayyil Veedu: Investigation, Methodology, Writing – original draft. **Agata Hajda:** Resources, Writing – review & editing. **Joanna Olesiak-Bańska:** Funding acquisition, Resources, Supervision, Writing – review & editing. **Jérôme Wenger:** Conceptualization, Funding acquisition, Investigation, Methodology, Project administration, Supervision, Writing – original draft.

Declaration of competing interest

The authors declare that they have no known competing financial interests or personal relationships that could have appeared to influence the work reported in this paper.

Data availability

The data that support the findings of this study data are available from the corresponding author upon request.

Acknowledgments

This project has received funding from the European Research Executive Agency (REA) under the Marie Skłodowska-Curie Actions doctoral network program (grant agreement No 101072818) and Sonata Bis project from the National Science Center in Poland (2019/34/E/ST5/00276). The authors thank Julia Osmólska for taking parts to the preliminary experiments characterizing AuNCs with FCS.

References

[1] C. Joo, H. Balci, Y. Ishitsuka, C. Buranachai, T. Ha, Advances in single-molecule fluorescence methods for molecular biology, Annu. Rev. Biochem. 77 (2008) 51–76, https://doi.org/10.1146/annurev.biochem.77.070606.101543.
[2] Z. Farka, M.J. Mickert, M. Pastucha, Z. Mikušová, P. Skládal, H.H. Gorris, Advances in optical single-molecule detection: En route to supersensitive bioaffinity assays, Angew. Chem. Int. Ed. 59 (2020) 10746–10773, https://doi.org/10.1002/anie.201913924.
[3] T. Wohland, S. Maiti, R. Machan, An Introduction to Fluorescence Correlation Spectroscopy, IOP Publishing Ltd, 2020, https://doi.org/10.1088/978-0-7503-2080-1.
[4] E. Haustein, P. Schwille, Fluorescence correlation spectroscopy: novel variations of an established technique, Annu. Rev. Biophys. Biomol. Struct. 36 (2007) 151–169, https://doi.org/10.1146/annurev.biophys.36.040306.132612.
[5] E.L. Elson, Fluorescence correlation spectroscopy: past, present, future, Biophys. J. 101 (2011) 2855–2870, https://doi.org/10.1016/j.bpj.2011.11.012.
[6] J.J. Gooding, K. Gaus, Single-molecule sensors: challenges and opportunities for quantitative analysis, Angew. Chem. Int. Ed. 55 (2016) 11354–11366, https://doi.org/10.1002/anie.201600495.
[7] S. Goodwin, J.D. McPherson, W.R. McCombie, Coming of age: ten years of next-generation sequencing technologies, Nat. Rev. Genet. 17 (2016) 333–351, https://doi.org/10.1038/nrg.2016.49.
[8] T. Zimmermann, J. Marrison, K. Hogg, P. O'Toole, Clearing up the signal: spectral imaging and linear unmixing in fluorescence microscopy, in: S.W. Paddock (Ed.), Confocal Microsc. Methods Protoc, Springer, New York, NY, 2014, pp. 129–148, https://doi.org/10.1007/978-1-60761-847-8_5.
[9] U. Kettling, A. Koltermann, P. Schwille, M. Eigen, Real-time enzyme kinetics monitored by dual-color fluorescence cross-correlation spectroscopy, Proc. Natl. Acad. Sci. 95 (1998) 1416–1420, https://doi.org/10.1073/pnas.95.4.1416.
[10] K. Bacia, P. Schwille, Practical guidelines for dual-color fluorescence cross-correlation spectroscopy, Nat. Protoc. 2 (2007) 2842–2856, https://doi.org/10.1038/nprot.2007.410.
[11] M. Burkhardt, K.G. Heinze, P. Schwille, Four-color fluorescence correlation spectroscopy realized in a grating-based detection platform, Opt. Lett. 30 (2005) 2266–2268, https://doi.org/10.1364/OL.30.002266.
[12] S. Giri, E.A. Sykes, T.L. Jennings, W.C.W. Chan, Rapid screening of genetic biomarkers of infectious agents using quantum dot barcodes, ACS Nano 5 (2011) 1580–1587, https://doi.org/10.1021/nn102873w.
[13] J. Kim, M.J. Biondi, J.J. Feld, W.C.W. Chan, Clinical validation of quantum dot barcode diagnostic technology, ACS Nano 10 (2016) 4742–4753, https://doi.org/10.1021/acsnano.6b01254.
[14] B.D. Reed, M.J. Meyer, V. Abramzon, O. Ad, O. Ad, P. Adcock, F.R. Ahmad, G. Alppay, J.A. Ball, J. Beach, D. Belhachemi, A. Bellofiore, M. Bellos, J.F. Beltrán, A. Betts, M.W. Bhuiya, K. Blacklock, R. Boer, D. Boisvert, N.D. Brault, A. Buxbaum, S. Caprio, C. Choi, T.D. Christian, R. Clancy, J. Clark, T. Connolly, K.F. Croce, R. Cullen, M. Davey, J. Davidson, M.M. Elshenawy, M. Ferrigno, D. Frier, S. Gudipati, S. Hamill, Z. He, S. Hosali, H. Huang, L. Huang, A. Kabiri, G. Kriger, B. Lathrop, A. Li, P. Lim, S. Liu, F. Luo, C. Lv, X. Ma, E. McCormack, M. Millham, R. Nani, M. Pandey, J. Parillo, G. Patel, D.H. Pike, K. Preston, A. Pichard-Kostuch, K. Rearick, T. Rearick, M. Ribezzi-Crivellari, G. Schmid, J. Schultz, X. Shi, B. Singh, N. Srivastava, S.F. Stewman, T. Thurston, T.R. Thurston, P. Trioli, J. Tullman, X. Wang, Y.-C. Wang, E.A.G. Webster, Z. Zhang, J. Zuniga, S.S. Patel, A.D. Griffiths, A.M. van Oijen, M. McKenna, M.D. Dyer, J.M. Rothberg, Real-time dynamic single-molecule protein sequencing on an integrated semiconductor device, Science. 378 (2022) 186–192, https://doi.org/10.1126/science.abo7651.
[15] D. Garoli, H. Yamazaki, N. Maccaferri, M. Wanunu, Plasmonic nanopores for single-molecule detection and manipulation: toward sequencing applications, Nano Lett. 19 (2019) 7553–7562, https://doi.org/10.1021/acs.nanolett.9b02759.
[16] J.R. Fries, L. Brand, C. Eggeling, M. Köllner, C.A.M. Seidel, Quantitative identification of different single molecules by selective time-resolved confocal fluorescence spectroscopy, J. Phys. Chem. A 102 (1998) 6601–6613, https://doi.org/10.1021/jp980965t.
[17] J. Widengren, V. Kudryavtsev, M. Antonik, S. Berger, M. Gerken, C.A.M. Seidel, Single-molecule detection and identification of multiple species by multiparameter fluorescence detection, Anal. Chem. 78 (2006) 2039–2050, https://doi.org/10.1021/ac0522759.
[18] M. Grabolle, P. Kapusta, T. Nann, X. Shu, J. Ziegler, U. Resch-Genger, Fluorescence lifetime multiplexing with nanocrystals and organic labels, Anal. Chem. 81 (2009) 7807–7813, https://doi.org/10.1021/ac900934a.
[19] M.S. Frei, M. Tarnawski, M.J. Roberti, B. Koch, J. Hiblot, K. Johnsson, Engineered HaloTag variants for fluorescence lifetime multiplexing, Nat. Methods 19 (2022) 65–70, https://doi.org/10.1038/s41592-021-01341-x.
[20] M. Böhmer, M. Wahl, H.-J. Rahn, R. Erdmann, J. Enderlein, Time-resolved fluorescence correlation spectroscopy, Chem. Phys. Lett. 353 (2002) 439–445, https://doi.org/10.1016/S0009-2614(02)00044-1.
[21] P. Kapusta, M. Wahl, A. Benda, M. Hof, J. Enderlein, Fluorescence lifetime correlation spectroscopy, J. Fluoresc. 17 (2007) 43–48, https://doi.org/10.1007/s10895-006-0145-1.
[22] P. Kapusta, R. Macháň, A. Benda, M. Hof, Fluorescence lifetime correlation spectroscopy (FLCS): concepts, applications and outlook, Int. J. Mol. Sci. 13 (2012) 12890–12910, https://doi.org/10.3390/ijms131012890.
[23] A. Ghosh, N. Karedla, J.C. Thiele, I. Gregor, J. Enderlein, Fluorescence lifetime correlation spectroscopy: basics and applications, Methods. 140–141 (2018) 32–39, https://doi.org/10.1016/j.ymeth.2018.02.009.

[24] D.C. Lamb, A. Schenk, C. Röcker, C. Scalfi-Happ, G.U. Nienhaus, Sensitivity enhancement in fluorescence correlation spectroscopy of multiple species using time-gated detection, Biophys. J. 79 (2000) 1129–1138, https://doi.org/10.1016/S0006-3495(00)76366-1.
[25] A. Benda, M. Hof, M. Wahl, M. Patting, R. Erdmann, P. Kapusta, TCSPC upgrade of a confocal FCS microscope, Rev. Sci. Instrum. 76 (2005) 033106, https://doi.org/10.1063/1.1866814.
[26] S. Rüttinger, P. Kapusta, M. Patting, M. Wahl, R. Macdonald, On the resolution capabilities and limits of fluorescence lifetime correlation spectroscopy (FLCS) measurements, J. Fluoresc. 20 (2010) 105–114, https://doi.org/10.1007/s10895-009-0528-1.
[27] C.T. Yuan, C.A. Lin, T.N. Lin, W.H. Chang, J.L. Shen, H.W. Cheng, J. Tang, Probing the photoluminescence properties of gold nanoclusters by fluorescence lifetime correlation spectroscopy, J. Chem. Phys. 139 (2013) 234311, https://doi.org/10.1063/1.4848695.
[28] J. Enderlein, I. Gregor, Using fluorescence lifetime for discriminating detector afterpulsing in fluorescence-correlation spectroscopy, Rev. Sci. Instrum. 76 (2005) 033102, https://doi.org/10.1063/1.1863399.
[29] J. Yao, D.R. Larson, H.D. Vishwasrao, W.R. Zipfel, W.W. Webb, Blinking and nonradiant dark fraction of water-soluble quantum dots in aqueous solution, Proc. Natl. Acad. Sci. 102 (2005) 14284–14289, https://doi.org/10.1073/pnas.0506523102.
[30] A.I. Bachir, D.L. Kolin, K.G. Heinze, B. Hebert, P.W. Wiseman, A guide to accurate measurement of diffusion using fluorescence correlation techniques with blinking quantum dot nanoparticle labels, J. Chem. Phys. 128 (2008) 225105, https://doi.org/10.1063/1.2918273.
[31] B.R. Fisher, H.-J. Eisler, N.E. Stott, M.G. Bawendi, Emission intensity dependence and single-exponential behavior in single colloidal quantum dot fluorescence lifetimes, J. Phys. Chem. B 108 (2004) 143–148, https://doi.org/10.1021/jp035756+.
[32] K.E. Knowles, E.A. McArthur, E.A. Weiss, A multi-timescale map of radiative and nonradiative decay pathways for excitons in CdSe quantum dots, ACS Nano 5 (2011) 2026–2035, https://doi.org/10.1021/nn2002689.
[33] E.B. Ureña, M.P. Kreuzer, S. Itzhakov, H. Rigneault, R. Quidant, D. Oron, J. Wenger, Excitation enhancement of a quantum dot coupled to a plasmonic antenna, Adv. Mater. 24 (2012) OP314–OP320, https://doi.org/10.1002/adma.201202783.
[34] M. Kayyil Veedu, J. Osmólska, A. Hajda, J. Olesiak-Banska, J. Wenger, Unveiling the photoluminescence dynamics of gold nanoclusters with fluorescence correlation spectroscopy, Nanoscale Adv. (2023), https://doi.org/10.1039/D3NA00869J.
[35] M.F. Matus, H. Häkkinen, Understanding ligand-protected noble metal nanoclusters at work, Nat. Rev. Mater. 8 (2023) 372–389, https://doi.org/10.1038/s41578-023-00537-1.
[36] M. Walter, J. Akola, O. Lopez-Acevedo, P.D. Jadzinsky, G. Calero, C.J. Ackerson, R. L. Whetten, H. Grönbeck, H. Häkkinen, A unified view of ligand-protected gold clusters as superatom complexes, Proc. Natl. Acad. Sci. 105 (2008) 9157–9162, https://doi.org/10.1073/pnas.0801001105.
[37] Z. Liu, Z. Wu, Q. Yao, Y. Cao, O.J.H. Chai, J. Xie, Correlations between the fundamentals and applications of ultrasmall metal nanoclusters: recent advances in catalysis and biomedical applications, Nano Today 36 (2021) 101053, https://doi.org/10.1016/j.nantod.2020.101053.
[38] M. Zhou, X. Du, H. Wang, R. Jin, The critical number of gold atoms for a metallic state nanocluster: resolving a decades-long question, ACS Nano 15 (2021) 13980–13992, https://doi.org/10.1021/acsnano.1c04705.
[39] Q. Li, M. Zhou, W.Y. So, J. Huang, M. Li, D.R. Kauffman, M. Cotlet, T. Higaki, L. A. Peteanu, Z. Shao, R. Jin, A mono-cuboctahedral series of gold Nanoclusters: photoluminescence origin, large enhancement, wide tunability, and structure–property correlation, J. Am. Chem. Soc. 141 (2019) 5314–5325, https://doi.org/10.1021/jacs.8b13558.
[40] C.M. Aikens, Electronic and geometric structure, optical properties, and excited state behavior in atomically precise thiolate-stabilized noble metal nanoclusters, Acc. Chem. Res. 51 (2018) 3065–3073, https://doi.org/10.1021/acs.accounts.8b00364.
[41] J. Olesiak-Banska, M. Waszkielewicz, P. Obstarczyk, M. Samoc, Two-photon absorption and photoluminescence of colloidal gold nanoparticles and nanoclusters, Chem. Soc. Rev. 48 (2019) 4087–4117, https://doi.org/10.1039/C8CS00849C.
[42] Z.-J. Guan, J.-J. Li, F. Hu, Q.-M. Wang, Structural engineering toward gold nanocluster catalysis, Angew. Chem. Int. Ed. 61 (2022) e202209725, https://doi.org/10.1002/anie.202209725.
[43] Y. Zhu, H. Qian, R. Jin, Catalysis opportunities of atomically precise gold nanoclusters, J. Mater. Chem. 21 (2011) 6793–6799, https://doi.org/10.1039/C1JM10082C.
[44] A. Thakran, A. Nain, M. Kataria, C.R. Paul Inbaraj, H.-Y. Lin, H.-I. Lin, Y.-M. Liao, C.-F. Hou, C.-C. Wang, H.-T. Chang, Y.-F. Chen, Highly efficient photodetection in metal nanocluster/graphene heterojunctions, ACS Photonics 8 (2021) 2955–2965, https://doi.org/10.1021/acsphotonics.1c00885.
[45] Y.-C. Chao, K.-P. Cheng, C.-Y. Lin, Y.-L. Chang, Y.-Y. Ko, T.-Y. Hou, C.-Y. Huang, W. H. Chang, C.-A.J. Lin, Non-toxic gold nanoclusters for solution-processed white light-emitting diodes, Sci. Rep. 8 (2018) 8860, https://doi.org/10.1038/s41598-018-27201-x.
[46] M.A. Abbas, T.-Y. Kim, S.U. Lee, Y.S. Kang, J.H. Bang, Exploring interfacial events in gold-nanocluster-sensitized solar cells: insights into the effects of the cluster size and electrolyte on solar cell performance, J. Am. Chem. Soc. 138 (2016) 390–401, https://doi.org/10.1021/jacs.5b11174.
[47] S. Qian, Z. Wang, Z. Zuo, X. Wang, Q. Wang, X. Yuan, Engineering luminescent metal nanoclusters for sensing applications, Coord. Chem. Rev. 451 (2022) 214268, https://doi.org/10.1016/j.ccr.2021.214268.
[48] M. Yu, J. Zhou, B. Du, X. Ning, C. Authement, L. Gandee, P. Kapur, J.-T. Hsieh, J. Zheng, Noninvasive staging of kidney dysfunction enabled by renal-clearable luminescent gold nanoparticles, Angew. Chem. 128 (2016) 2837–2841, https://doi.org/10.1002/ange.201511148.
[49] Y. Chen, D.M. Montana, H. Wei, J.M. Cordero, M. Schneider, X. Le Guével, O. Chen, O.T. Bruns, M.G. Bawendi, Shortwave infrared in vivo imaging with gold nanoclusters, Nano Lett. 17 (2017) 6330–6334, https://doi.org/10.1021/acs.nanolett.7b03070.
[50] P. Obstarczyk, A. Pniakowska, M.P. Nonappa, J. Olesiak-Bańska Grzelczak, Crown ether-capped gold nanoclusters as a multimodal platform for bioimaging, ACS Omega. 8 (2023) 11503–11511, https://doi.org/10.1021/acsomega.3c00426.
[51] A. Pniakowska, J. Olesiak-Banska, Plasmonic enhancement of two-photon excited luminescence of gold nanoclusters, Molecules. 27 (2022) 807, https://doi.org/10.3390/molecules27030807.
[52] K. Klehs, C. Spahn, U. Endesfelder, S.F. Lee, A. Fürstenberg, M. Heilemann, Increasing the brightness of cyanine fluorophores for single-molecule and superresolution imaging, ChemPhysChem. 15 (2014) 637–641, https://doi.org/10.1002/cphc.201300874.
[53] J. Maillard, K. Klehs, C. Rumble, E. Vauthey, M. Heilemann, A. Fürstenberg, Universal quenching of common fluorescent probes by water and alcohols, Chem. Sci. 12 (2021) 1352–1362, https://doi.org/10.1039/D0SC05431C.
[54] H. Deng, K. Huang, L. Xiu, W. Sun, Q. Yao, X. Fang, X. Huang, H.A.A. Noreldeen, H. Peng, J. Xie, W. Chen, Bis-Schiff base linkage-triggered highly bright luminescence of gold nanoclusters in aqueous solution at the single-cluster level, Nat. Commun. 13 (2022) 3381, https://doi.org/10.1038/s41467-022-30760-3.
[55] J. Goetz, A. Nonat, A. Diallo, M. Sy, I. Sera, A. Lecointre, C. Lefevre, C.F. Chan, K.-L. Wong, L.J. Charbonnière, Ultrabright lanthanide nanoparticles, ChemPlusChem. 81 (2016) 526–534, https://doi.org/10.1002/cplu.201600007.
[56] M. Sy, A. Nonat, N. Hildebrandt, L.J. Charbonnière, Lanthanide-based luminescence biolabelling, Chem. Commun. 52 (2016) 5080–5095, https://doi.org/10.1039/C6CC00922K.
[57] C. Charpentier, V. Cifliku, J. Goetz, A. Nonat, C. Cheignon, M. Cardoso Dos Santos, L. Francés-Soriano, K.-L. Wong, L.J. Charbonnière, N. Hildebrandt, Ultrabright terbium nanoparticles for FRET biosensing and in situ imaging of epidermal growth factor receptors**, Chem. Eur. J. 26 (2020) 14602–14611, https://doi.org/10.1002/chem.202002007.